**Paper CIT06-0681**

# LARGE EDDY SIMULATION OF A FLOW OVER A BACKWARD-FACING STEP USING A CVFEM-FORMULATION

**Rosiane Cristina de Lima[1]**
rosiane@ita.br
[1] Instituto Tecnológico de Aeronáutica, Departamento de Engenharia Aeronáutica e Mecânica, Área de Aerodinâmica, Propulsão e Energia – Praça Marechal Eduardo Gomes, 50, Vila das Acácias, CEP 12228-900, São José dos Campos, SP

**João Batista Campos Silva[2]**
jbcampos@dem.feis.unesp.br
[2] UNESP-Faculdade de Engenharia de Ilha Solteira, Departamento de Engenharia Mecânica, Área de Ciências Térmicas, Av. Brasil, 56 – Ilha Solteira -SP

*Abstract: The turbulent flow over a backward-facing step has been investigated by many researchers due to its several applications in engineering problems, as: diffusers, airfoils with separation, buildings, combustors and turbines blades. This problem is largely used to validate numerical codes due to simplicity geometric. It's important to supply data that can be used to ascertain turbulence models, wall laws and their implementation in computational codes. The main goal of this work is to verify the performance of the large-eddy methodology, which was implemented in a nine-node CVFEM-code. In this case none wall law was utilized. The domain is discretized using nine-node finite elements and the equations are integrated into control volumes around the nodes of the finite elements. The Navier-Stokes equations are filtered for large scale simulations and the sub-grid scale stress, which appear due to the filtering process, are modeled by the eddy viscosity model of Smagorinsky. The principal parameter evaluated in this problem is the reattachment length value and the appearing of a secondary recirculation at the corner eddy. The results are compared to experimental data available in the literature presenting good agreement.*

*Keywords: backward-facing step, numerical simulation, CVFEM, large eddy simulation, Smagorinsky sub-grid model*

## 1. Introduction

The main goal of this work is to simulate numerically turbulent flow over a backward-facing step by a control volume finite element method (CVFEM) with large-eddy simulation methodology (LES). The computational domain is discretized with nine-node quadrilateral finite elements.

The first CVFEM was presented by Baliga and Patankar (1980) for triangular elements and afterwards Raw and Schneider (1986) used the method, therefore using quadrilateral elements. Since then, several other authors have improved and applied the CVFEM in a vast number of problems in engineering.

Saabas (1991) developed a CVFEM to solve steady state flow problems in multi-dimensional domains using three-node triangular elements and four-node tetrahedron elements. According to the author CVFEM offers the combination of geometric flexibility of the finite element method (FEM) and the ease of physical interpretation associated with the commonly used Finite Volume Method (FVM).

Recently, Lima, Campos-Silva and Mansur (2004) enhanced the CVFEM code built by Campos-Silva (1998) including a Large Eddy Simulation (LES) methodology with the Smagorinsky viscosity model to simulate turbulent fluid flows. In that work the authors presented a lid-driven cavity using nine-node quadrilateral elements to discretize the domain presenting excellent agreement to literature results.

The first applications on LES in engineering were present by Deardorff (1970), in the investigation of a turbulent flow inside a channel with high Reynolds number. Initially, LES was used to performer basic flows in simple geometries; however, due to the rapid development of computational power, it has been applied to practical engineering flows in relatively complex geometries (Hamba, 2003; Löhner, 2001).

In this study will be analyzed the turbulent flow over a backward-facing step. Such problem has been investigated by many researchers due to its several applications in engineering problems, as: diffusers, airfoils with separation, buildings, combustors and turbines blades. According to Eaton and Johnston (1981), who performed an experimental study about this case, the backward-facing step offers one of the least complex separating and reattaching flows. The separation line of the backward-facing step flow is straight and fixed at the step edge; therefore the process of separation-reattachment can be examined without any complexities resulting from motion of the separation point. There is only one separated flow zone with two opposing eddies.

The main parameters evaluated in the step flow are the reattachment length value ($L_R/h$) and the appearing of a secondary recirculation at corner eddy. The results are compared to numerical and experimental results from literature.

In next sections of this work, it will be reported the mathematical model, a summary about the used numerical method, the problem description and the obtained results.

## 2. Mathematical Model

### 2.1 Governing Equations

The following equations set describe the mathematical modeling of a turbulent fluid flow, with constant properties. According to Lima (2005) the dimensionless equations for large-eddy simulation are:

$$\frac{\partial U_i}{\partial t} + \frac{\partial (U_j U_i)}{\partial X_j} = -\frac{\partial P_t}{\partial X_i} + \frac{\partial}{\partial X_j}\left(\left(\frac{1}{\text{Re}} + \nu_t\right)\frac{\partial U_i}{\partial X_j}\right) + \frac{\partial}{\partial X_j}\left(\nu_t \frac{\partial U_j}{\partial X_i}\right) + F_i \tag{1}$$

$$\frac{\partial U_i}{\partial X_i} = 0 \tag{2}$$

The pressure term in Eq. (1) includes the kinetic turbulent energy, $P_t = \overline{P} + \frac{2}{3}\frac{k}{u_0^2}$.

The dimensionless variables, in Eqs. (1) and (2), are defined as follows:

$$X_i = \frac{x_i}{L} \; ; \; U_i = \frac{u_i}{u_0} \; ; \; \overline{P} = \frac{p - p_0}{\rho u_0^2} \; ; \; t = \frac{t^*}{L/u_0} \; ; \; \nu_t = \frac{\nu_t^*}{u_0 L} = \left(C_s \frac{\Delta}{L}\right)^2 \left(2\overline{S}_{kl}\overline{S}_{kl}\right)^{1/2} \; ; \; \text{Re} = \frac{\rho u_0 L}{\mu} \tag{3}$$

where,

| | |
|---|---|
| $C_s$: | Smagorinsky constant; |
| L: | reference length; |
| p, $p_0$: | static pressure and reference pressure, respectively; |
| t: | non-dimensional time; |
| $u_0$: | reference velocity; |
| $U_i$: | velocities; |
| $X_i$: | coordinates; |
| μ: | dynamic fluid viscosity; |
| $\nu_t$: | kinematics turbulent fluid viscosity; |
| ρ: | fluid density; |
| Δ: | filter width; |
| *: | dimensional variables. |

In the large-eddy simulation methodology the physical quantities such as velocity and pressure are decomposed in large grid-scale (LGS) and sub-grid scale (SGS) components through a filtering process. The filter function used in this case was set be equal to the length of a control volume face where are considered the convective and diffusive fluxes. The filter function most common is the filter function by volume. The filter width, $\Delta$, is generally defined as: $\Delta = \left(\Delta_x \Delta_y \Delta_z\right)^{1/3}$ in 3D and $\Delta = \left(\Delta_x \Delta_y\right)^{1/2}$ in 2D problems with $\Delta_{x_i}$ being the grid size in the $x_i$-axis. In the following section it will be presented the numerical technique used in this work.

## 3. Numerical Method

The formulation of control-volume finite element method (CVFEM) involves five basic steps, Saabas and Baliga (1994a, 1994b): (1) discretization of the domain into finite elements; (2) another discretization of the domain into control volumes, which surround the nodes of the finite element mesh; (3) definition of element-based interpolation functions for variables and physical properties of the fluid; (4) derivation of algebraic equations by using

the sub-domain weighted residual method; and (5) assembling of the element equations creating the global matrix and the choice of a procedure to compute the system of algebraic equations.

**Figure 1** illustrates a nine-node finite element, control volumes and integration points (Ip) at faces of control volumes inside an element. The continue lines, the bold points, dashed lines and arrows represent the finite element contour, the nodal points, the control volumes contours and fluxes direction respectively. It can be noticed that each nodal point is inside a control volume like in finite volume method (FVM) and the integrations are done in counter-clockwise rotation.
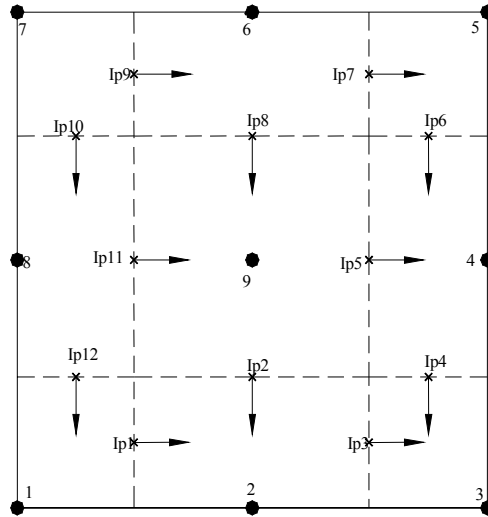


Figure 1 – Finite element divided in control volumes and integration points.

In order to simplify the integration process, each element in global coordinates (x,y), (Figure 2a), is mapped in a master element in local coordinates ($\xi,\eta$), (Figure 2b). So, all the nodal points of the integration domain are definite in the range [-1, 1], which is primordial to apply the integration Gaussian quadrature rule. However, it also must be done a further mapping to each control volume area and contour inside elements.



Figure 2 (a) - Element in global coordinates (x,y).  Figure 2 (b) – Master element in local coordinates ($\xi,\eta$).
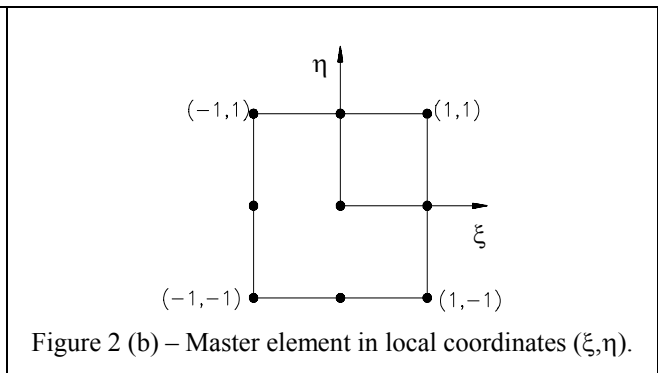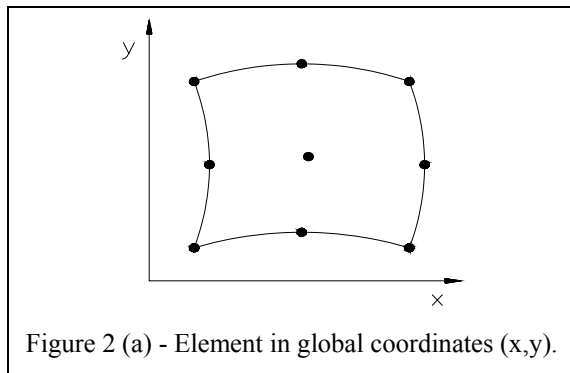
Thus, the integrals in areas defined by $\int_{\xi_1}^{\xi_2} \int_{\eta_1}^{\eta_2} f(\xi,\eta)d\xi d\eta$ can be calculated by $\int_{-1}^{1}\int_{-1}^{1} g(r,s)drds$, which facilitates the integration process. Integrals in contours are of the type $\int_{\xi_1}^{\xi_2} f(\xi)d\xi$ or $\int_{\eta_1}^{\eta_2} f(\eta)d\eta$, may be calculated as the definite integral in the range [-1, 1], $\int_{-1}^{1} g(s)ds$.

In this way, the coefficient matrices are computed element by element in local coordinates and a global system of equations is assembled like in the classical finite element method. In this work have been used nine Gauss points for integration in areas to exactly integrate the mass matrix and three Gauss points for integration along contours. After the assembling, the algebraic global system of equations in the matrix notation is as follow:

$$K(U)U = F \tag{4}$$

where it can be seen that the global matrix *K* depends on the global vector of unknown parameters (U), this occurs due to the non-linearity of the inertia terms. Iterative successive substitutions were employed to solve Eq. (4) until the convergence is attained.

The global system of equations is solved by the frontal method developed by Taylor and Hughes (1981). In this method the global system never is totally assembled in the computer memory. So, personal computers may be used to solve large problems (with more nodal points or degree of freedom).

Following, is presented the integration process in each control volume. Integrating Eqs. (1) and (2), ones obtain for each element:

$$\int_\Omega \frac{\partial U_i}{\partial t}\,d\Omega + \oint_\Gamma \left( U_j U_i - \left( \frac{1}{Re} + \nu_t \right) \frac{\partial U_i}{\partial X_j} \right) n_j\,d\Gamma + \int_\Omega \frac{\partial P_t}{\partial X_i}\,d\Omega = \oint_\Gamma \nu_t \frac{\partial U_j}{\partial X_i} n_j\,d\Gamma + \int_\Omega F_i\,d\Omega \tag{5}$$

$$\int_\Omega \frac{\partial U_i}{\partial X_i}\,d\Omega = 0 \tag{6}$$

where $\Omega$ and $\Gamma$ are symbols for area and contour of a control volume around a node inside elements, respectively. The arrows in Figure 1 indicate the outward normal vector to the contour of a control volume, $n_j$, in which there are convective and diffusive fluxes. This normal vector for integration in the counter-clockwise direction has been defined as: $\vec{n}dS = n_1\,dS\vec{i} + n_2\,dS\vec{j} = dy\vec{i} - dx\vec{j}$ .

In order to transform the integrals of Eqs. (5) and (6) into algebraic equations, the variables in those integrals must be interpolated by appropriate functions. In this study the variables and coordinates are interpolated by Lagrangian interpolation functions. The variables inside each element are interpolated as:

$$U^e(X(\xi,\eta),Y(\xi,\eta),t) = \sum_{\alpha=1}^{nnep} N_\alpha(\xi,\eta)U_\alpha(t) \tag{7}$$

$$V^e(X(\xi,\eta),Y(\xi,\eta),t) = \sum_{\alpha=1}^{nnep} N_\alpha(\xi,\eta)V_\alpha(t) \tag{8}$$

$$P^e(X(\xi,\eta),Y(\xi,\eta),t) = \sum_{\lambda=1}^{nnel} N_\lambda(\xi,\eta)P_\lambda(t) \tag{9}$$

$$X^e(\xi,\eta) = \sum_{\alpha=1}^{nnep} N_\alpha(\xi,\eta)X_\alpha \tag{10}$$

$$Y^e(\xi,\eta) = \sum_{\alpha=1}^{nnep} N_\alpha(\xi,\eta)Y_\alpha \tag{11}$$

where, according to Dhatt and Touzot (1984),

| | |
|---|---|
| $\alpha$ : | interpolation nodes for the velocities; |
| $\lambda$ : | interpolation nodes for the pressure; |
| $N_\alpha$ and $N_\lambda$ : | interpolation functions; |
| nnep and nnel: | node numbers for quadratic (parabolic) and linear elements, respectively; |
| $P_\lambda$ : | nodal pressure; |
| $U_\alpha$ and $V_\alpha$ : | nodal values of velocity components; |
| $X_\alpha$ and $Y_\alpha$ : | coordinates at the node α of the elements. |

After the replacement of Eqs. (7)-(9) into Eqs. (5) and (6) ones obtain the set of algebraic equations:

$$M_{\alpha\beta}\dot{U}_{i\beta} + C_{\alpha\beta}(U_{i\beta})U_{i\beta} - S_{i\alpha\beta}U_{i\beta} + H_{i\alpha\beta}P_\beta = F_{i\alpha} \tag{12}$$

$$D_{i\alpha\beta}U_{i\beta} = 0 \tag{13}$$

where $M_{\alpha\beta}$, $C_{\alpha\beta}$, $S_{i\alpha\beta}$, $H_{i\alpha\beta}$, $D_{i\alpha\beta}$ and $F_{i\beta}$ are mass coefficients, convection, diffusive, pressure term, continuity matrices and the source term vector, respectively, for each element. The detailed definition for these matrices can be founded in Campos-Silva (1998).

After the discretization of the transient term $\dot{U}_{i\beta}$ of Eqs. (12) and (13) are obtained the following algebraic equations:

$$\frac{M_{\alpha\beta}}{\Delta t}U_{i\beta}^{n+1} + \theta(C_{\alpha\beta}^{n+1} - S_{i\alpha\beta})U_{i\beta}^{n+1} + \theta H_{i\alpha\beta}P_{\beta}^{n+1} =$$

$$\frac{M_{\alpha\beta}}{\Delta t}U_{i\beta}^{n} - (1-\theta)(C_{\alpha\beta}^{n} - S_{i\alpha\beta})U_{i\beta}^{n} - (1-\theta)H_{i\alpha\beta}P \tag{14}$$

$$D_{i\alpha\beta}U_{i\beta}^{n+1} = 0 \tag{15}$$

where the time discretization parameter ($\theta$) is in the range [0, 1]. In the present work was employed the fully implicit scheme, $\theta = 1$. In this case is not necessary the usage of any initial condition for the pressure field.

## 4. Results

Following are presented the simulations done for a classical benchmark problem: a flow over the backward-facing step. Despite the simplicity geometrical it presents a substantial complexity in its flows due to the appearing of a recirculation zone, which posses two opposite vortex.

The main goal of this study is to verify the capability of a turbulence model implemented in an in-house code to predict the dependent features of the backward-facing step problem (Figure 3) as: reattachment length and corner eddy recirculation. These results are function of independent parameters as: initial boundary layer state, the initial boundary layer thickness, free stream turbulence, pressure gradient and aspect ratio.

The geometrical configuration and boundary conditions, for this challenge case, are shown in Figure 3. The inflow is placed -1.33h upstream of the step (with h=step height). The outflow is located about 28h downstream of the step. Two cases were performed in this study with different velocity profiles at the inflow ($U_0$). In the first and second case were imposed parabolic and uniform velocity profile conditions at the inflow, respectively. A set of null pressure was forced at the exit boundary and a set of null velocities was imposed at the remaining walls. In both cases the square of the Smagorinsky constant was set to $C_s^2 = 0.0324$.



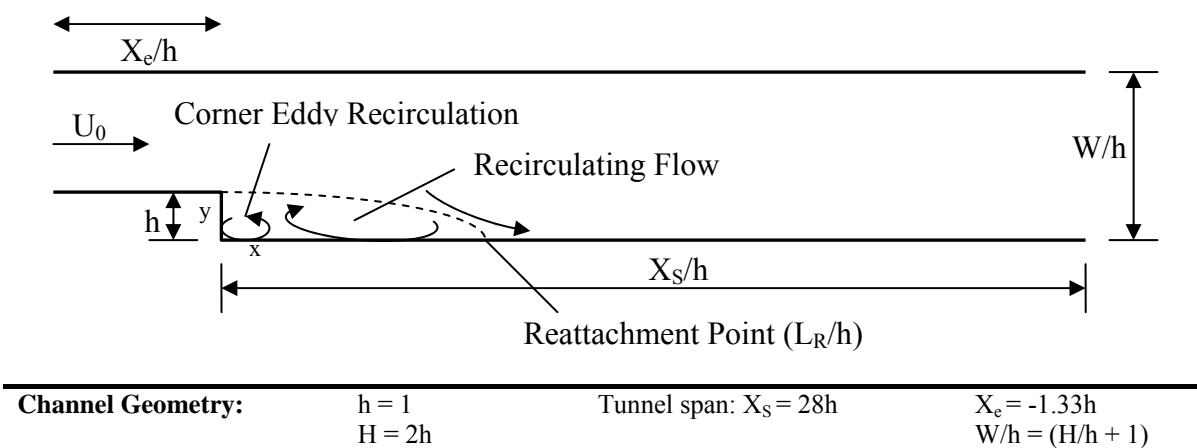| Channel Geometry: | h = 1 | Tunnel span: $X_S$ = 28h | $X_e$ = -1.33h |
|---|---|---|---|
| | H = 2h | | W/h = (H/h + 1) |

Figure 3– Computational domain and boundary conditions of the flow in a sudden expansion of a channel.

Figure 4 presents a slice of the computational domain discretized by a non-uniform quadratic nine-node finite elements; this grid was used for both the cases. This mesh amount 2,550 elements (or 10,413 grid points) and 23,483 degrees of freedom, which correspond to 13 by 51 and 121 by 81 nodal points at the entrance and in the tunnel span of the channel, respectively.

Figure 4 – Slice of the computational domain of the backward facing step discretized in 13 by 51 (entrance) and 121 by 81 (tunnel span) grid points.

In Table 1 are showed the boundary conditions for the backward facing step with parabolic velocity profiles in the entrance. The coordinate R has been started in the middle point of the inlet. The calculations have been performed for Reynolds numbers of 73 and 229.

Table 1 – Boundary conditions for the backward facing step with parabolic velocity profile in the entrance.

| | | |
|---|---|---|
| **Inlet Conditions:** | $U_o = 1.33(1 - R^2)$ <br> $-1 \leq R \leq 1$ | $Re_h=73$ <br> $Re_h=229$ |
| **Outlet Conditions:** | p=0 | |
| **Channel Walls:** | u=v=0 | |

Figures 5-6 show velocity profiles for Reynolds number equal to 73 along of the channel. The results were compared to Winterscheidt and Surana (1994) and Campos-Silva (1998). In this second work wasn't used none turbulence model, however it can be noted that for this Reynolds number there isn't a substantial influence of the turbulence model, so the results present good agreement.
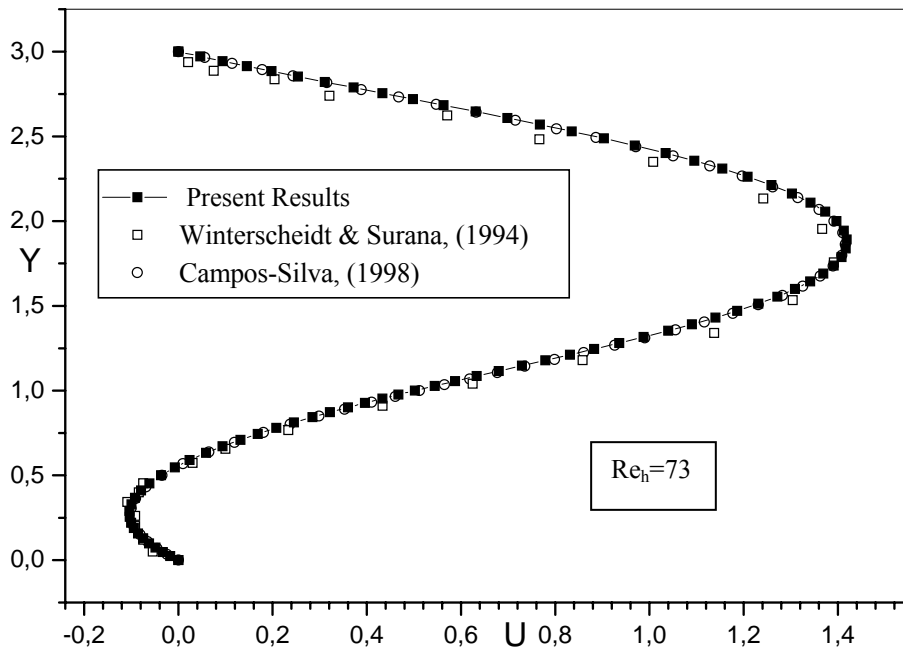


Figure 5 – U-velocity profiles at the downstream of the backward facing step (X/h=2).
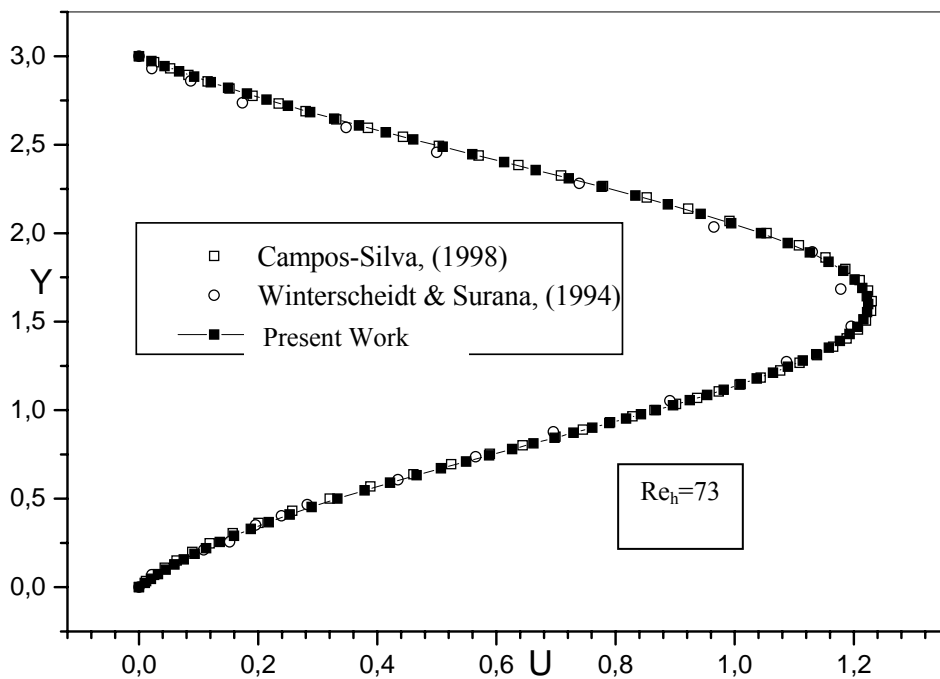
Figure 6 - U-velocity profiles at the downstream backward facing step (X/h=6).

Velocity profiles for Reynolds number equal to 229 in two points in downstream of the step (X/h=2 and X/h=6) were compared to Winterscheidt and Surana (1994); Figure 7 enlightens this comparison, which present good agreement.
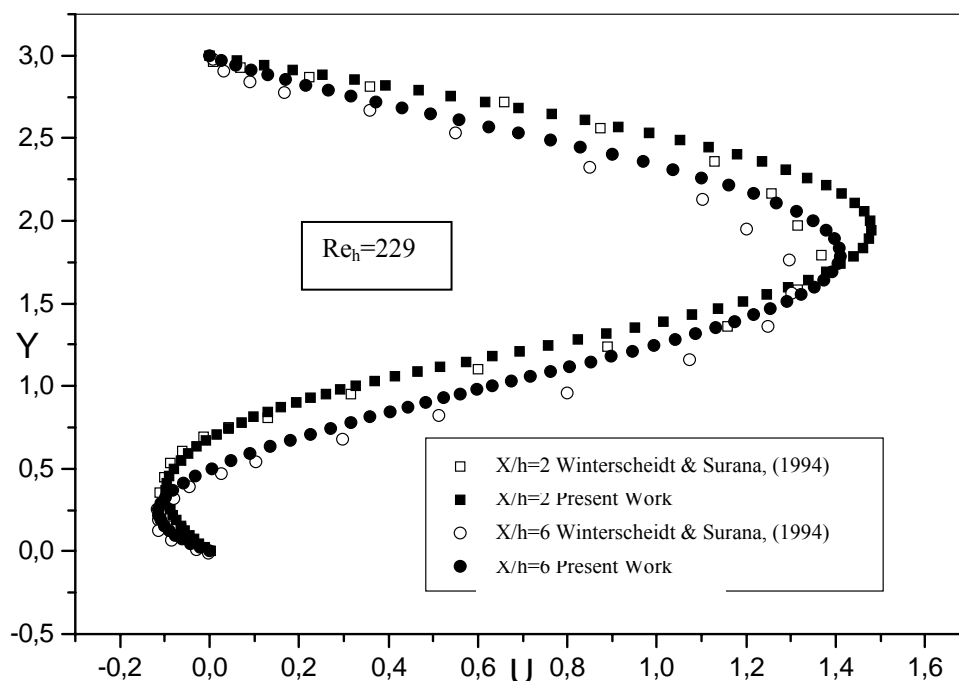


Figure 7 - U-velocity profiles at the downstream of the step.

**Table 2** shows the reattachment point for the Reynolds number 73 and 229. The results were compared to numerical (B and C columns) and experimental (A column) values. The experimental value was extract to

Winterscheidt & Surana (1994). The results of this work (D column) presented a small deviation (E column), below 14%.

Table 2 – Reattachment point ($L_R/h$) for the Reynolds numbers 73 and 229.

| $Re_h$ | A<br>Experimental | B<br>Campos-Silva<br>(1998) | C<br>Winterscheidt &<br>Surana (1994) | D<br>Present<br>Work | E<br>$|[(C-D)*100]/C|$ |
|--------|-------------------|------------------------------|----------------------------------------|----------------------|------------------------|
| **73** | 4.0 | 5.0 | 5.3 | 5.9 | 11.3% |
| **229** | | 9.7 | 9.7 | 11.0 | 13.4% |

Following are presented results which posses uniform velocity profile condition in the inflow of the step flow. Table 3 presents the boundary conditions and Reynolds number imposed in this case.

Table 3 - Boundary conditions for the backward facing step with uniform velocity profile in the entrance.

| | | |
|---|---|---|
| **Inlet Conditions:** | $U_0 = 1$ | $10,000 \leq Re_h \leq 71,000$ |
| **Outlet Conditions:** | $p=0$ | |
| **Channel Walls:** | $u=v=0$ | |

The results presented are of calculations performed for Reynolds numbers of 10,000, 14,000, 45,000 and 71,000. Initially, it was simulated the case for $Re_h = 2,000$ with intention to use their velocity profiles as initial condition for $Re_h=10,000$, which would be used as initial condition for $Re_h=14,000$ and so on, this procedure assisted in the convergence process.

The numerical values ($L_R/h=7.3$) obtained in the present study for all Reynolds numbers simulated shows an excellent agreement to experimental results ($L_R/h=7 \pm 1$) by Kim et al (1978). Thought the results can be noted that the flow apparently becomes independent of the Reynolds number when the boundary layer is fully turbulent, this also was observed by Eaton and Johnston (1981).

The streamlines are exhibited in the Figures 8-11 for Reynolds numbers of 10,000, 14,000, 45,000 and 71,000, respectively. The streamlines become possible the visualization of the separation line of the flow over the backward-facing step, which is straight and fixed at the downstream of the step. There is only one separated flow zone with two opposing eddies.
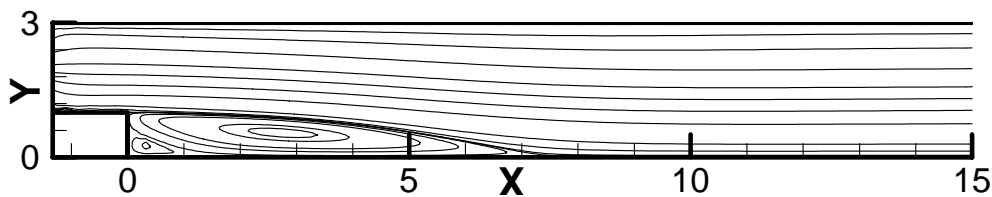


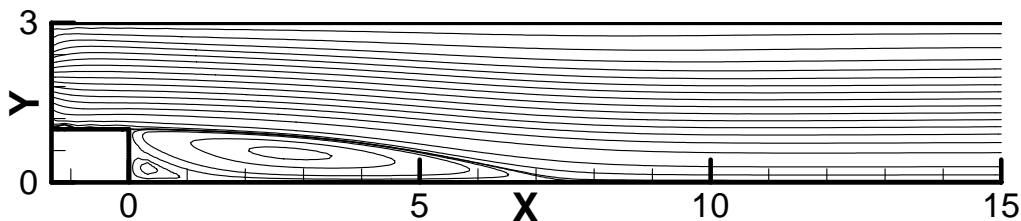Figure 8 - Streamlines in a sudden expansion of a channel for $Re_h=10,000$.



Figure 9 - Streamlines in a sudden expansion of a channel for $Re_h=14,000$.
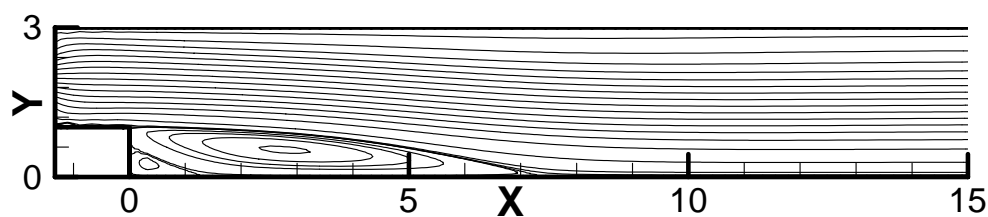
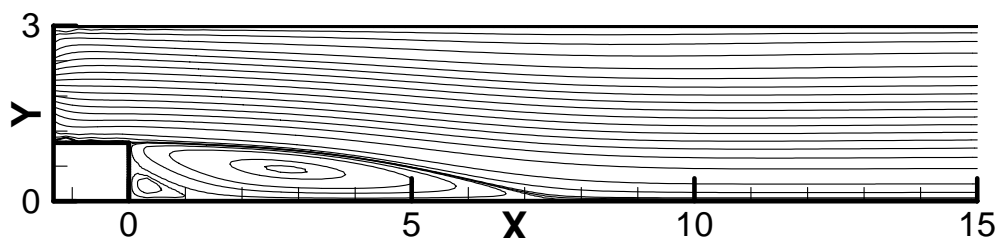Figure 10 - Streamlines in a sudden expansion of a channel for $Re_h$=45,000.



Figure 11 - Streamlines in a sudden expansion of a channel for $Re_h$=71,000.

## 5. Conclusions

In the present work were presented large-eddy simulations by a control volume–finite element or sub-domain finite element method using nine-node finite elements with quadratic and linear interpolation functions for velocity and pressure fields, respectively. The benchmark problem backward-facing step flows have been solved on Pentium 4 personal computer, 2 GHz and 2 Gb of RAM. Despite, no upwind technique has been applied and the fully implicit first order method has been used for time discretization the results present excellent agreement to results available from the literature.

In the flow over a backward facing step two principal parameters are evaluated: reattachment length values (a comparison can be view in Table 2) and the appearing of the corner eddy recirculation, which can be noted in Figures 8 -11. Both the results present good agreement to the literature.

## 6. Acknowledgement

## 7. References

Baliga, B. R. and Patankar, S. V., 1980, "A new finite-element formulation for convection-diffusion problems", Numerical Heat Transfer, vol. 3., pp. 393-409.

Campos Silva, J. B., 1998, "Numerical simulation of fluid flow by the finite element method based on control volumes", Doctorate Thesis (in Portuguese), State University of Campinas, Campinas, São Paulo, Brazil.

Deardorff, J. W., 1970, "A numerical study of tri-dimensional turbulent channel flow at large Reynolds number", Journal Fluids Mechanics, 41, 342-379 pp.

Dhatt, G. and Touzot, G., 1984, "The Finite Element Method Displayed", John Wiley and Sons Ltda, New York, 526 p.

Eaton, J.K. and Johnston, J.P., 1981, "A review of research on subsonic turbulent flow reattachment", AIAA Journal, Vol. 19, No. 9, 1093-1100 pp.

Hamba, F., 2003, "A Hybrid RANS/LES Simulation of Turbulent Channel Flow". Theoretical and Computational Fluid Dynamics, vol. 16, pp. 387–403.

Kim, J., Kline, J., Johnston, J.P., 1978, "Investigation of Separation and Reattachment of a Turbulent Shear Layer: Flow Over a Backward-Facing Step", Report MD-37, Thermosciences Division, Department of Mechanical Engineering, Stanford University, Stanford.

Lima, R. C., Mansur, S. S. and Campos Silva, J. B., 2004, "Large Eddy Simulation of Turbulent Incompressible Fluid Flows by a Nine-Nodes Control Volume-Finite Element Method", Proc. X Brazilian Congress of Thermal Sciences and Engineering - ENCIT'04, Rio de Janeiro/RJ, 29/11/04 a 03/12/2004, paper code 0636.

Lima, R. C., 2005, "Large-eddy simulation incompressible fluid flows with heat and mass transfer by a sub-domain finite element method" (In Portuguese)., Master Dissertation, São Paulo State University, (UNESP-Ilha Solteira), Ilha Solteira, S.P., Brazil, 161 p.

Löhner, R., 2001, "Applied computational fluid dynamics techniques – An introduction based on finite element methods". John Wiley and Sons Ltd, New York, 376 p.

Raw, M. J. and Schneider, G. E., 1986, "A skewed, positive influence coefficient up-winding procedure for control-volume-based finite-element convection-diffusion computation", Numerical Heat Transfer, vol. 9, pp. 1-26.

Saabas, H. J., 1991, "A control volume finite element method for three-dimensional, incompressible, viscous fluid flow", Ph.D. Thesis, Dept. of. Mech. Eng., McGill University, Montreal, Que, Canada.

Saabas, H. J. and Baliga, B. R., 1994a, "Co-located equal-order control-volume finite-element method for multidimensional, incompressible, fluid flow - Part I: Formulation", Numerical Heat Transfer, Part B, vol. 26, pp.381-407.

Saabas, H. J. and Baliga, B. R., 1994b, "Co-located equal-order control-volume finite-element method for multidimensional, incompressible, fluid flow - Part II: Verification", Numerical Heat Transfer, Part B, vol. 26, pp.409-424.

Taylor, C. and Hughes, T. G., 1981, "Finite Element Programming of the Navier-Stokes Equations", Pineridge Press Ltd, Swansea, U.K.

Winterscheidt, D. and Surana, K.S., 1994, "p-Version Least Squares Finite Element Formulation for Two-Dimensional, Incompressible Fluid Flow", Int. J. Numer. Methods Fluids, vol. 18, p.43-69.

## 8. Copyright Notice